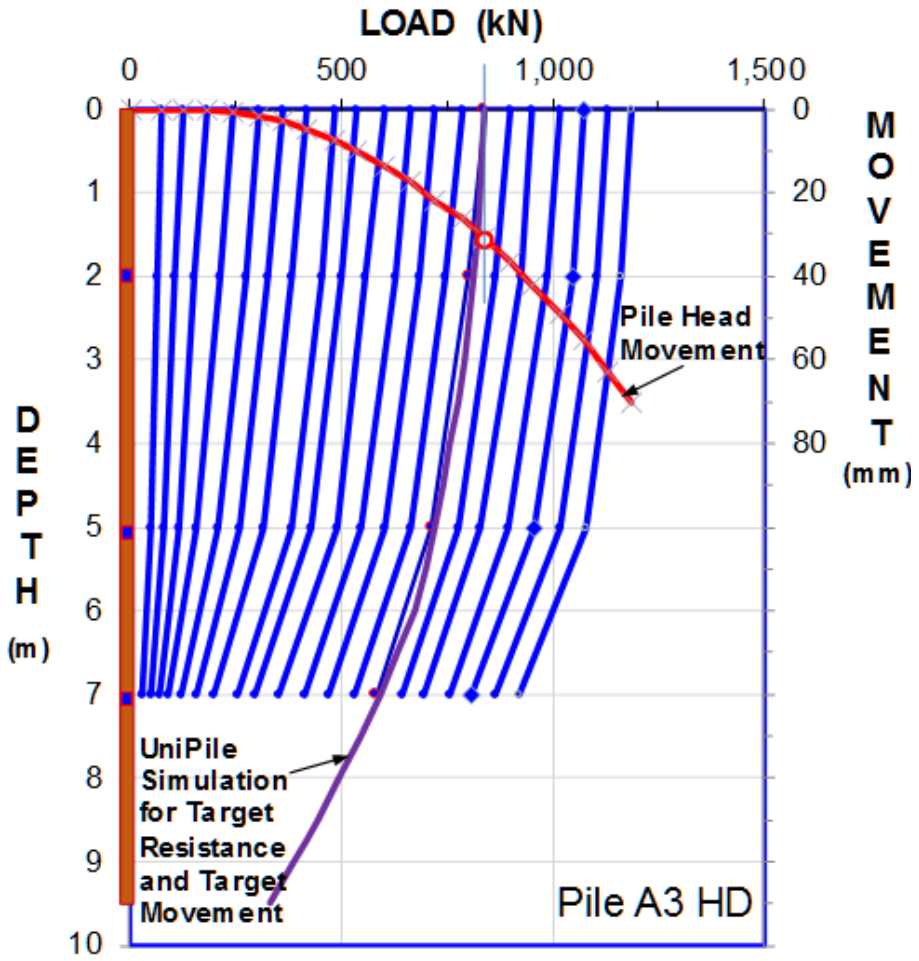

380. Fellenius, B.H., 2017. Summary and comments on my prediction to the 3rd CFPB. Proceedings of the 3rd Bolivian International Conference on Deep Foundations, Santa Cruz de la Sierra, Bolivia, April 27-29, Vol. 3, pp. 73-81.

Summary and comments on my prediction to the 3rd CFPB

Fellenius, B.H.[(1)]

[(1)] Consulting Engineer, Sidney, BC, Canada, V8L 2B9. <bengt@fellenius.net>

ABSTRACT. The analysis method used to produce the predictions and to back-calculate the actual test results is based on load-movement characteristics of the pile-soil interface carried out using a set of t-z/q-z functions characterized by a target point, which is a point on the resistance-movement curve determined by a target resistance and a target movement. The resistance curve is then defined by a t-z or q-z function controlled by a single function-specific coefficient. The analysis input and the predicted and actual pile responses are presented.

1. SOIL PROFILE

The site investigation at the B.E.S.T. site, the soil exploration, notably the CPTU sounding results, show the soil profile to consist of essentially two soil layers: an upper 6 m thick layer of loose silt and sand on compact silty sand. The CPTU pore pressure measurements indicated a groundwater table near or about 0.5-m depth and a hydrostatically distributed pore pressure. Figure 1 shows a diagram compiling the SPT N-indices and the CPTU cone stress, q_t. Results of pressuremeter and dilatometer test can be obtained from the conference website: www.cfpbolivia.com.

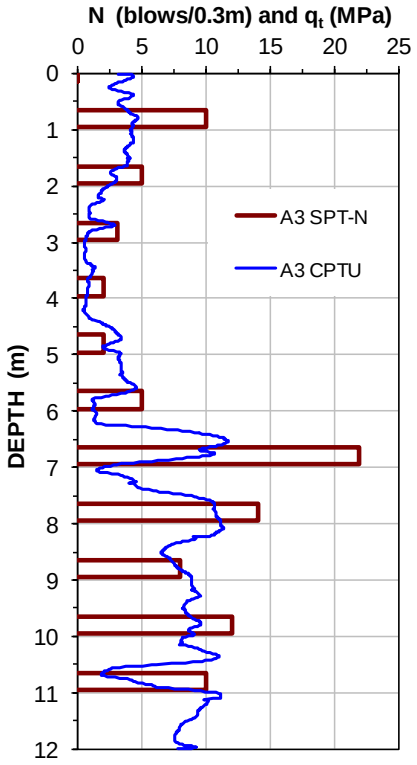

Fig. 1. SPT N-indices compiled with the CPTU q_t-stress at Pile A3.

2. ANALYSIS PRINCIPLES

Several methods based on in-situ tests are available for calculating the response to load applied to a single pile. For example, based on the cone penetrometer test: the Dutch CPT-method (DeRuiter and Beringen 1976), the Schmertmann CPT-method (Schmertmann 1978), the LCPC CPT-method (Bustamante and Gianeselli 1982), and the Eslami-Fellenius CPTU-method (Eslami and Fellenius 1997). Based on the standard penetration test: the three most commonly referenced methods are by Meyerhof (1976), Decourt (1999), and O'Neill and Reese (1999). There are also methods based on pressuremeter and dilatometer tests.

The aspects in common for all the methods based on results of in-situ tests are that they were originally referenced (calibrated) to a capacity determined from the results of actual tests. No consideration appears to have been included about the movement of the pile head (or pile toe) at the so-assessed capacities, nor was anything reported about how that reference capacity was defined and the shape of the particular pile-head load-movement curves before and after the "capacity". Indeed, for many 'calibrations', there was no distinction made what portion of the resistance was from the shaft and what from the toe.

Figure 2 shows the distribution of axial load in test pile A3 calculated using the mentioned seven in-situ methods. The actually measured pile-head load and the back-calculated distribution (addressed below) are also shown along with, the pile head load-movement curve (note, the movement is per the right side ordinate). Figure 3 shows the shaft resistance distribution for the same records.

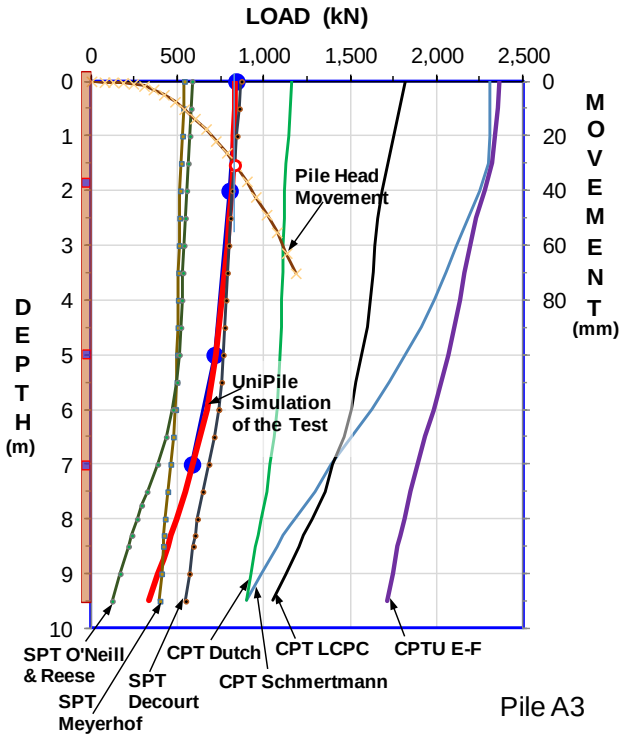

Fig. 2. Axial load distribution.

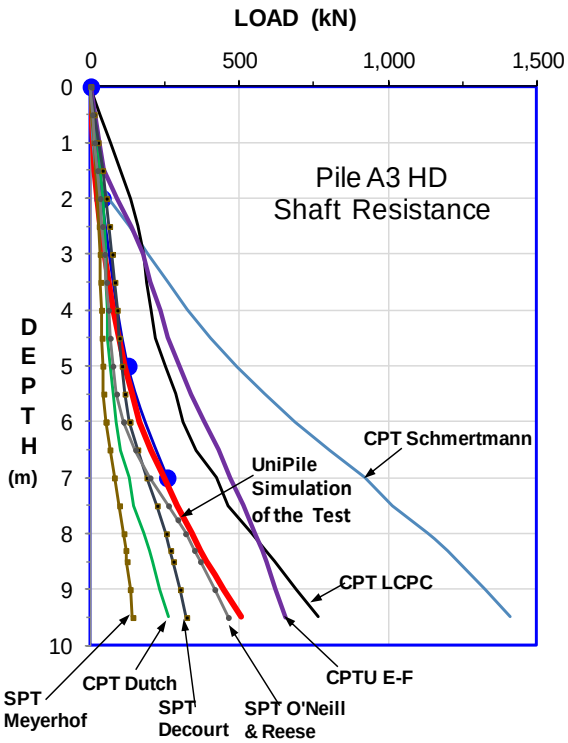

Fig. 3. Distributions of shaft resistance.

The response of pile to an applied load is by transferring the axial load to the soil by shaft and toe resistances, which both increase with increasing relative movement. The stiffness, i.e., the slope of the resistance versus shear, depends on the surrounding stress, expressed as overburden effective stress, and on the shear stiffness. That is, the shaft resistance along a specific pile element or toe resistance for a pile toe element are functions of the effective overburden stress and the relative movement between the pile and the soil at the element considered. The relations can take on different shapes and be continually increasing, reach a certain value and then stay constant or decrease—strain-hardening, plastic, or strain-softening—, as illustrated in Figure 4. The figure depicts six different curves of resistance versus movement, each following a distinct mathematical relation. Such curves are called *t-z* or *q-z* functions.

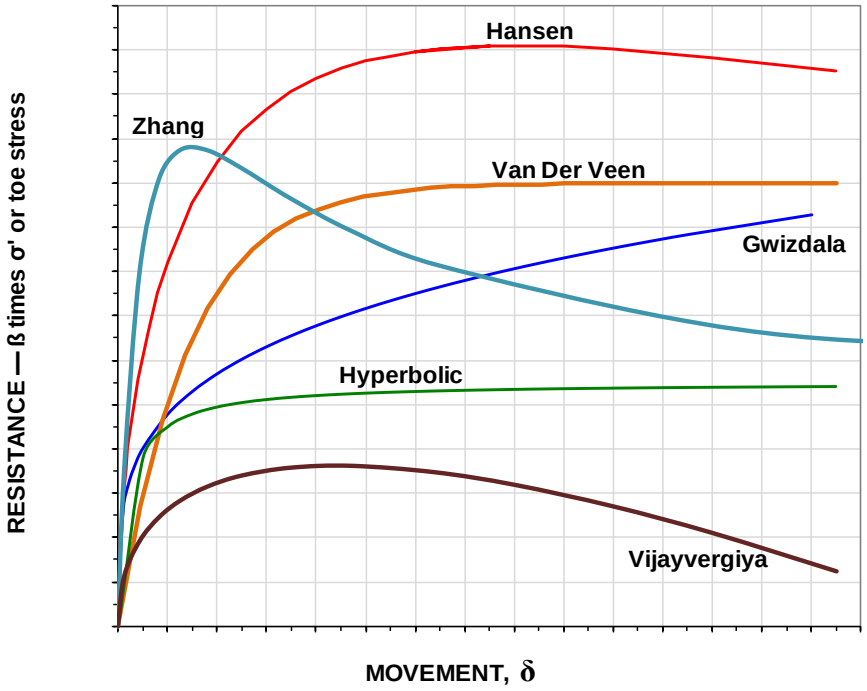

Fig. 4. Six resistance versus movement curves.

Three of the curves shown in the figure, Hansen (1963), Zhang (2012), and Vijayvergiya (1977), rise to a maximum value, a peak, and decay thereafter. One, Vander Veen (1953); also called "exponential function"), rises to a maximum and then stays constant—plastic behavior. Two curves, the Gwizdala (1996; also called "ratio function") and Chin-Kondner Hyperbolic (Chin 1970), continue to increase with increasing movement. The value of the maximum resistances—when there—and the shapes and movements differ between the curves. I have detailed the functions and equations in my 'Red Book" textbook (Fellenius 2017).

Both shaft and toe resistance are usually just referred to by a strength value, a certain proportionality coefficient, called beta (*ß*) times the effective stress acting at the element (or, more primitively, by a strength value directly, in total stress analysis). However, that value is not meaningful unless the movement at which it is mobilized is also noted and, moreover, also the shape before and after this resistance-movement point on the curve.

Figure 5 shows the six functions adjusted to pass through a common resistance-movement point. For the Vijayvergiya, Hansen, and Vander Veen functions, it would be kind of logical to call the assigned common point the "capacity" of the element. Not so, however, for the Zhang curve which has a peak resistance that is larger than that of the point and for the Gwizdala curve for which the point is no more characteristic than any other point on the curve. Therefore, I prefer to use the terms "target point", "target resistance", and "target movement". Any actual resistance-movement response of a pile element can be described by reference to the target point and coupled with the equation for the curve that best models the response—shape—before and after the target point. N.B., for the application of a *t-z/q-z* curve, the development after the target point, the shape, is very important. The shape is determined by a single coefficient, unique to each of the six *t-z* functions. While shaft resistance (*t-z*) can follow any of the six functions, the toe response function (called *q-z* function) rarely follows any other than the Gwizdala function.

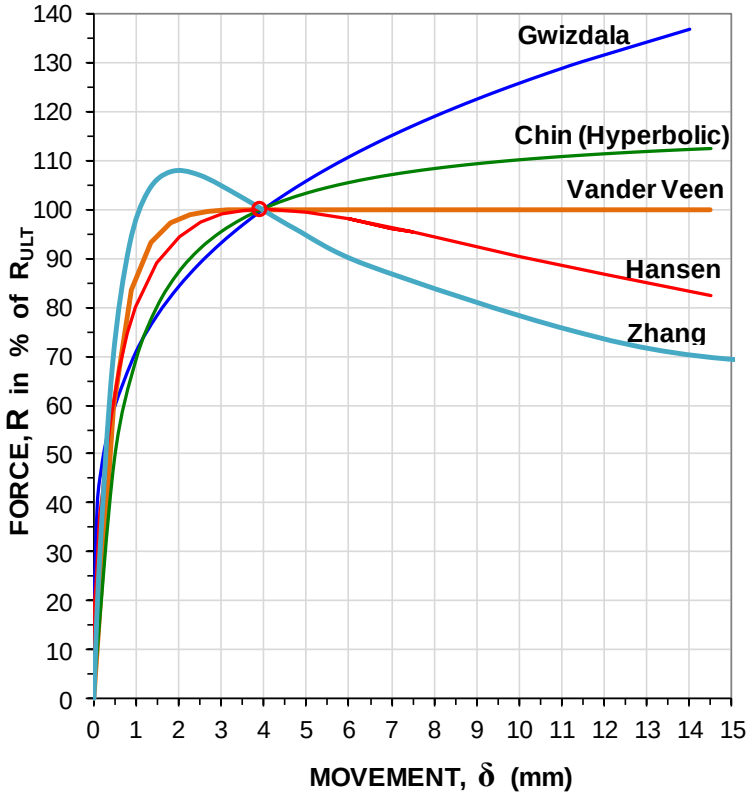

Fig. 5. The six *t-z/q-z* curves passing through a common point.

Whether for a design of a piled foundation, a prediction of a pile response to load, or a back-analysis of a static loading test, the analysis starts by choosing a target point for the pile element response—one for the entire length of pile or one for each particular soil layer—and combining this with a suitable *t-z* function to choose the shape of the resistance-movement before and after the target point. Of course, the analysis must also incorporate the other particulars of the soil profile, such as soil density, depth to the groundwater table, and pore pressure distribution.

Table 1 shows the calculation input for my prediction of the load-movement response of Pile A3.

TABLE 1. Input parameters for prediction analysis of Pile A3.

Parameter	Upper Layer	Lower layer
Depth range (m)	0 to 6.0	6.0 to 10.0
Density (kg/m^3)	2,000	2,100
Target *ß*-coefficient	0.3	0.4
Target toe stress (kPa)		1,500
Target movement (mm)	30	30
t-z function	Vander Veen	Gwizdala
t-z coefficient	0.40	0.20
q-z function		Gwizdala
q-z coefficient		0.60

The pile was a 620-mm diameter, 9.5 m long, slurry-constructed, bored concrete pile with a 30-GPa axial *E*-modulus.

In selecting the input, I referred to the results of the previous tests in Santa Cruz carried out in connection with the 1st and 2nd CFPB. I derived no numerical support from the site investigation data and the selected the input shown in Table 1 by "engineering judgment".

The analysis was carried out using the UniPile software (Goudreault and Fellenius 2014). The beta and toe-stress input resulted in a 940-kN total target resistance at the 30-mm target toe movement. As the calculated pile shortening was 0.85 mm, the pile head movement was 30.85 mm for the target values.

Table 2 compiles the input used in UniPile to back-calculate the actual results. The fit uses slightly larger target beta-coefficients and smaller target toe resistance than those used for the prediction. The back-calculation target movement was the same as that used for the prediction.

TABLE 2. Input parameters adjusted in back-calculation.

Parameter	Upper Layer	Lower layer
Target ß-coefficient	0.4	0.6
Target toe stress (kPa)		1,100
t-z function	Vander Veen	Hyperbolic
t-z coefficient	2.00	0.0070
q-z function		Gwizdala
q-z coefficient		0.70

Figure 6 presents the *t-z* and *q-z* curves for the prediction and to the curves used in UniPile's calculations of the load-movement curves for the back-calculation of the measured response of Pile A3. At each curve, the *t-z*/*q-z* curve 100 % ordinate value is the unit shaft or toe resistances for the pile elements within the respective soil layers.

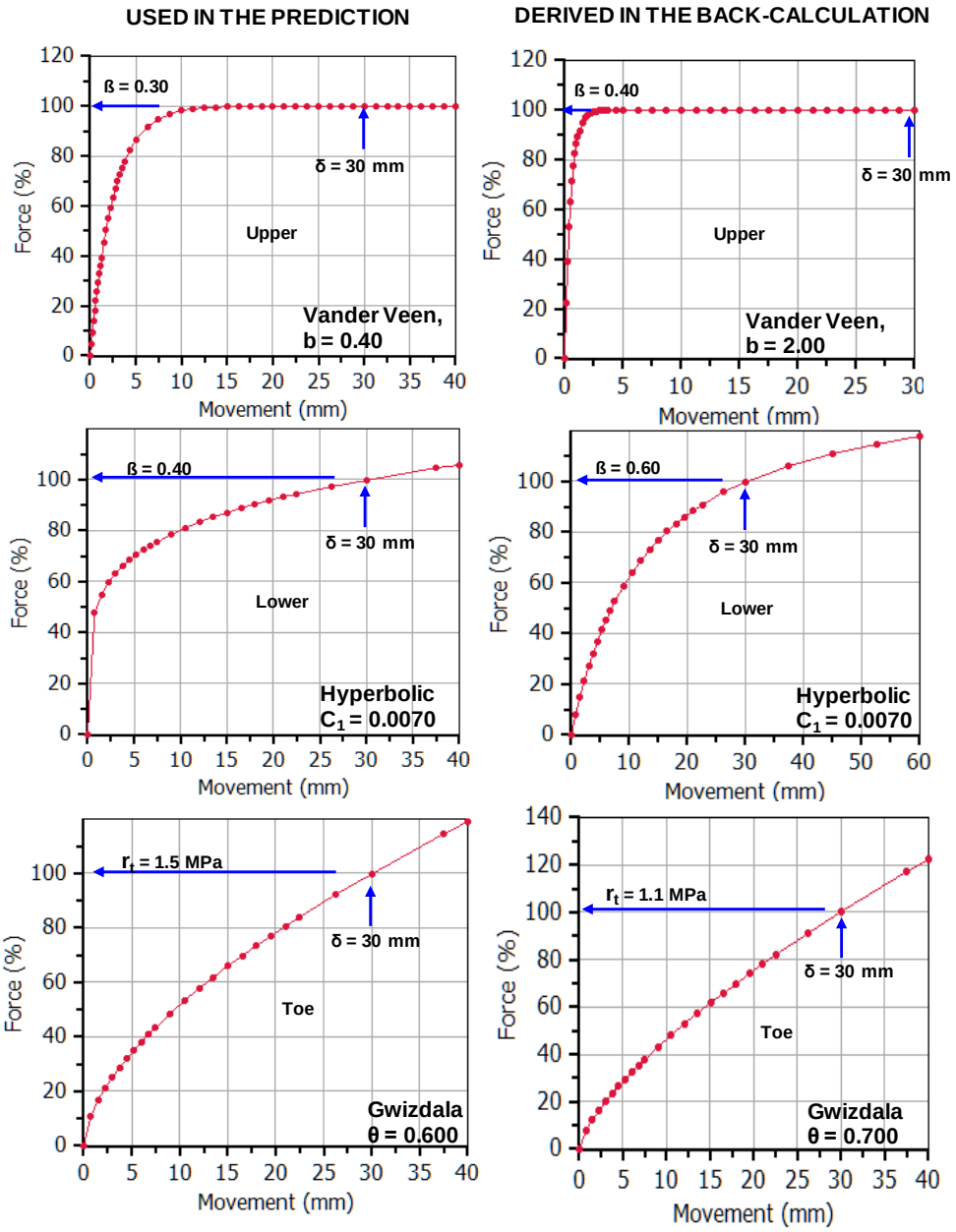

Fig. 6. Comparisons of *t-z/q-z* curves used in the prediction of Pile A3 load-movement response and as derived from a back-calculation of the actual test data.

Figure 7 shows the Pile A3 measured load-distribution (determined from the strain-gage instrumentation) and the back-calculated load distribution for the target resistance. For comparison, the figure also includes the load distribution resulting from the prediction input.

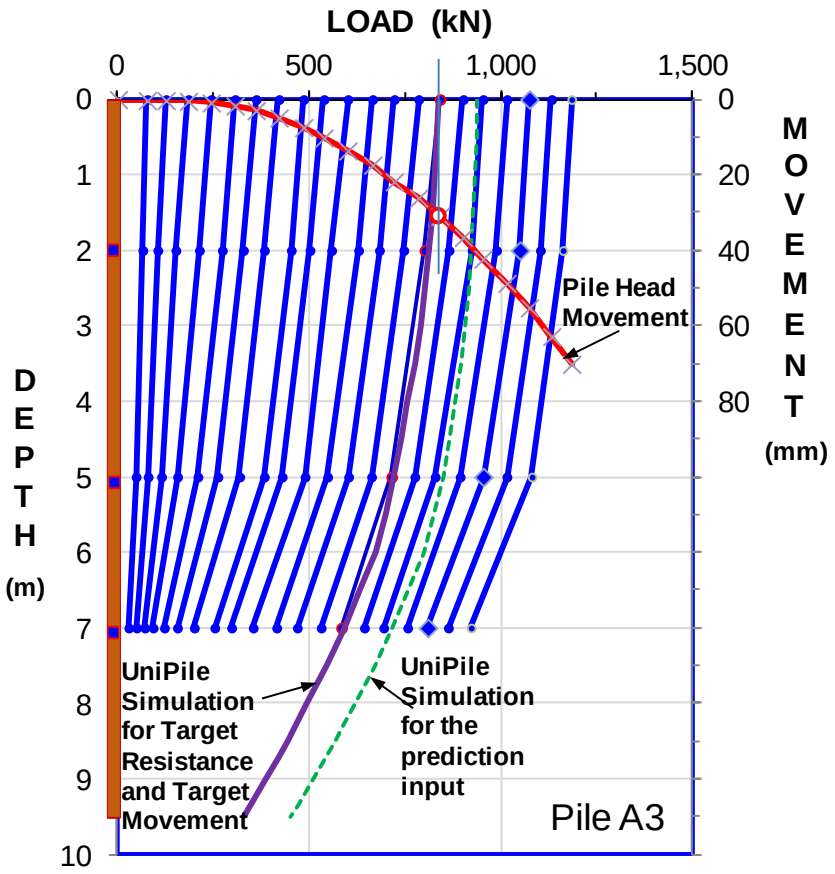

Fig. 7. Pile A3 measured and back-calculated load distribution.

Figure 8 shows the predicted, measured, and back-calculated pile-head load-movement curves for Pile A3. The back-calculation of the test was carried out by, first, choosing a target point on the test curve and finding which beta-coefficients and toe resistance that gave total resistance equal to the chosen target point. Then, potentially applicable *t-z* and *q-z* functions were tried and, for each, the coefficient was varied until calculated load-movement curves reasonably fitted the measured curve also before and after the target point. One or other function gave the best fit.

The agreement between the predicted and actual curves is quite good. As Figure 9 makes clear, the agreement of my predictions of the other two head-down tests included in the prediction event (Pile B2 and C2) with the actual test curve, is considerably less good. I obviously underestimated the improvement of the pile stiffness for the CFA and FDP construction methods for both the shaft and toe responses.

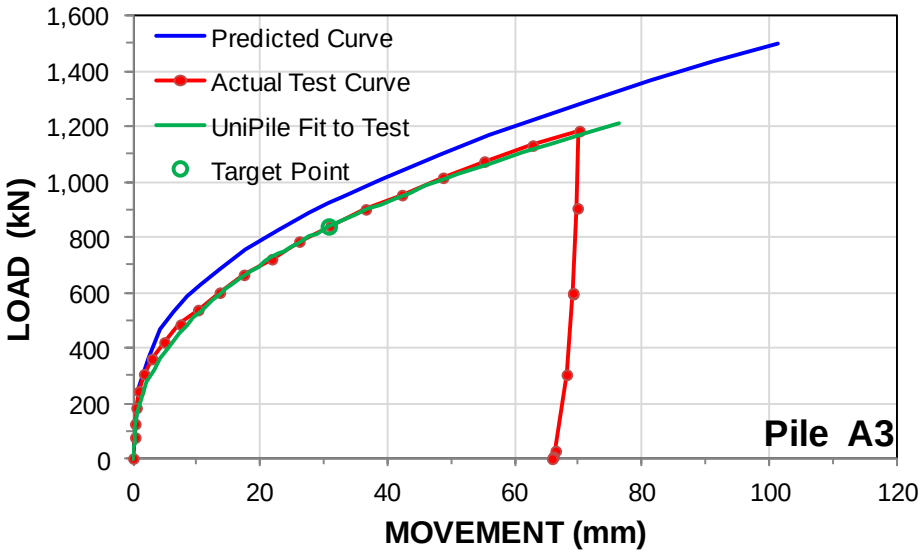

Fig. 8. Predicted, measured, and back-calculated load-movement curves for Pile A3.

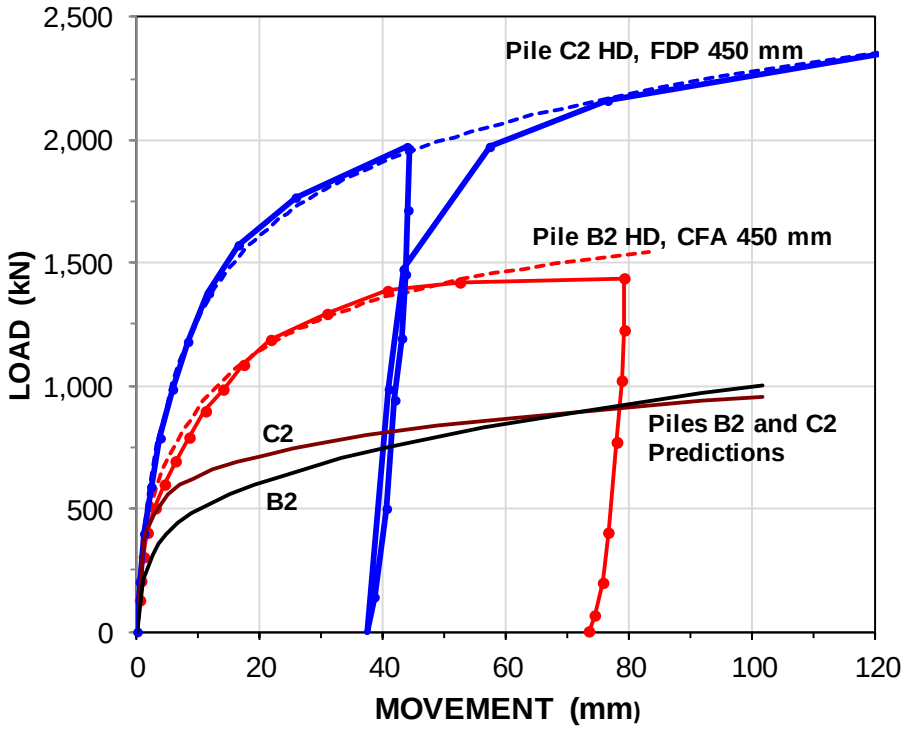

Fig. 9. Predicted, measured, and back-calculated load-movement curves for Piles B2 and C2.

The back-calculations fitting the UniPile analysis to the results of the tests show the power of the *t-z/q-z* computations in determining the load-movement response of pile. The success of a design of a piled foundation ultimately rests with the foundation settlement response to the applied load. What the particular capacity definition and resistance factor that happened to be used for the design is rather moot.

References

Bustamante, M. and Gianeselli, L., 1982. Pile bearing capacity predictions by means of static penetrometer CPT. Proc. of the Second European Symposium on Penetration Testing, ESOPT II, Amsterdam, May 24-27, A.A. Balkema, Vol. 2, pp. 493-500.

Chin, F.K., 1970. Estimation of the ultimate load of piles not carried to failure. Proc. of the 2nd Southeast Asian Conference on Soil Engineering, pp. 81-90.

Decourt, L., 1982. Prediction of bearing capacity of piles based exclusively on N-values of the SPT. Proc. ESOPT II, Amsterdam, May 24-27, pp. 19-34.

Decourt, L., 1999. Behavior of foundations under working load conditions. Proc. of 11th Pan-American Conference on Soil Mechanics and Geotechnical Engineering, Foz DoIguassu, Brazil, August 1999, Vol. 4, pp. 453 488.

DeRuiter, J. and Beringen F.L., 1979. Pile foundations for large North Sea structures. Marine Geotechnology, 3(3) 267 314.

Eslami, A. and Fellenius, B.H., 1997. Pile capacity by direct CPT and CPTu methods applied to 102 case histories. Canadian Geotechnical Journal 34(6) 886–904.

Fellenius, B.H., 2017. Basics of foundation design–a textbook. Pile Buck International, Inc., Vero Beach, FL, Electronic Edition. www.Fellenius.net, 464 p.

Goudreault, P.A. and Fellenius, B.H., 2014. UniPile Version 5, User and Examples Manual. UniSoft Geotechnical Solutions Ltd. [www.UniSoftLtd.com]. 120 p.

Gwizdala, K., 1996. The analysis of pile settlement employing load-transfer functions (in Polish). Zeszyty Naukowe No. 532, Budownictwo Wodne No.41, Technical University of Gdansk, Poland, 192 p.

Hansen, J.B., 1963. Discussion on hyperbolic stress-strain response. Cohesive soils. ASCE Journal for Soil Mechanics and Foundation Engineering, 89(SM4) 241-242.

Meyerhof, G.G., 1976. Bearing capacity and settlement of pile foundations. The Eleventh Terzaghi Lecture, November 5, 1975. ASCE Journal of Geotechnical Engineering 102(GT3), 195-228.

O'Neill, M.W. and Reese, L.C., 1999. Drilled shafts. Construction procedures and design methods, Federal Highway Administration, Transportation Research Board, Washington, FHWA-IF99-025.

Vander Veen, C., 1953. The Bearing Capacity of a Pile. Proc. of the 3rd ICSMFE, Zürich, Switzerland, August 16-27, Vol. 2, pp. 84-90.

Schmertmann, J.H., 1978. Guidelines for cone penetration test, performance, and design. U.S. Federal Highway Administration, Washington, Report FHWA-TS-78-209, 145 p.

Vijayvergiya, V.N., 1977. Load-movement characteristics of piles. Proc. of Port '77 Conference, ASCE, Long beach, Ca, March 9 - 11, Vol. 2, pp. 269-284.

Zhang Q.Q. and Zhang, Z.M., 2012. Simplified non-linear approach for single pile settlement analysis. Canadian Geotechnical Journal, 49(11). 1256-1266.